ORIGINAL ARTICLE – CANCER RESEARCH

CrossMark

Diverging impact of cell fate determinants Scrib and Llgl1 on adhesion and migration of hematopoietic stem cells

Banaja P. Dash[1] · Tina M. Schnöder[1,2] · Carolin Kathner[1,2] · Juliane Mohr[3,4] · Sönke Weinert[5] · Carolin Herzog[4] · Parimala Sonika Godavarthy[6] · Costanza Zanetti[6] · Florian Perner[1,2] · Rüdiger Braun-Dullaeus[5] · Björn Hartleben[7] · Tobias B. Huber[8,9,10] · Gerd Walz[9] · Michael Naumann[11] · Sarah Ellis[12] · Valera Vasioukhin[13] · Thilo Kähne[11] · Daniela S. Krause[6] · Florian H. Heidel[1,2]

Abstract

Purpose Cell fate determinants Scrib and Llgl1 influence self-renewal capacity of hematopoietic stem cells (HSCs). Scrib-deficient HSCs are functionally impaired and lack sufficient repopulation capacity during serial transplantation and stress. In contrast, loss of Llgl1 leads to increased HSC fitness, gain of self-renewal capacity and expansion of the stem cell pool. Here, we sought to assess for shared and unique molecular functions of Llgl1 and Scrib by analyzing their interactome in hematopoietic cells.

Methods Interactome analysis was performed by affinity purification followed by mass spectrometry. Motility, migration and adhesion were assessed on primary murine HSCs, which were isolated by FACS sorting following conditional deletion of Scrib or Llgl1, respectively. Imaging of Scrib-deficient HSCs was performed by intravital 2-photon microscopy.

Results Comparison of Scrib and Llgl1 interactome analyses revealed involvement in common and unique cellular functions. Migration and adhesion were among the cellular functions connected to Scrib but not to Llgl1. Functional validation of these findings confirmed alterations in cell adhesion and migration of Scrib-deficient HSCs in vitro and in vivo. In contrast, genetic inactivation of Llgl1 did not affect adhesion or migratory capacity of hematopoietic stem cells.

Conclusion Our data provide first evidence for an evolutionarily conserved role of the cell fate determinant Scrib in HSC adhesion and migration in vitro and in vivo, a unique function that is not shared with its putative complex partner Llgl1.

Keywords Cell fate determinants · Polarity · Scribble · Llgl1 · Migration · Adhesion · Hematopoietic stem cells · HSC

✉ Florian H. Heidel
  Florian.Heidel@med.uni-jena.de

1 Innere Medizin II, Hämatologie und Onkologie, Universitätsklinikum Jena, Am Klinikum 1, 07747 Jena, Germany

2 Leibniz Institute on Aging, Fritz-Lipmann Institute, Jena, Germany

3 Institute for Molecular and Clinical Immunology, Otto-von-Guericke University Medical Center, Magdeburg, Germany

4 Department of Hematology and Oncology, Otto-von-Guericke University Medical Center, Magdeburg, Germany

5 Department of Cardiology and Angiology, Otto-von-Guericke University Medical Center, Magdeburg, Germany

6 Institute for Tumor Biology and Experimental Therapy, Georg-Speyer-Haus, Frankfurt am Main, Germany

7 Institute of Pathology, Medizinische Hochschule Hannover, Hannover, Germany

8 III Department of Medicine, University Medical Center Hamburg-Eppendorf, Hamburg, Germany

9 Department of Medicine IV, Medical Center, University of Freiburg, Freiburg, Germany

10 BIOSS Center for Biological Signaling Studies, Albert-Ludwigs-University, Freiburg, Germany

11 Institute for Experimental Medicine, Otto-von-Guericke University Medical Center, Magdeburg, Germany

12 Cancer Research Division, Peter MacCallum Cancer Centre, Melbourne, Australia

13 Division of Human Biology, Fred Hutchinson Cancer Research Center, Seattle, WA, USA

Introduction

In drosophila the Scribble complex consists of Scribble (Scrib), Discs large (Dlg) and Lethal giant larvae (Lgl) and these complex partners are involved in regulation of intracellular and inter-cellular signaling. Thereby, the complex influences cellular responses and facilitates subsequent cell fate decisions. An important mechanism by which the Scribble complex regulates cell fate decisions is asymmetric cell division (ACD), which modulates polarity during cell division and results in the production of two daughter cells with different molecular properties (Knoblich 2010). Loss of cell polarity can influence tumor development, progression and metastasis, but may also affect stem cell function by its relevance for cell division processes (Humbert et al. 2008; Knoblich 2010). Cellular functions of the Scribble complex members have been studied in detail in drosophila organ development and cellular differentiation. In mammalian cells, several homologs of Dlg (Dlg1-4) and Lgl (Llgl1-2) exist while Scribble has none. Recent data suggests, that some cellular functions of the Scribble complex members are evolutionarily conserved in the mammalian system, however, they may vary depending on the underlying cell type or differentiation stage (Hawkins et al. 2013, 2014, 2016; Heidel et al. 2015; Humbert et al. 2008; Mohr et al. 2018; Sengupta et al. 2011). Recently, we and others provided the first evidence for a functional role of Llgl1 and Scrib in the self-renewal and maintenance of hematopoietic stem cells (Althoff et al. 2017; Heidel et al. 2013; Mohr et al. 2018). While genetic inactivation of Llgl1 led to increased fitness and self-renewal capacity of murine HSCs in vivo (Heidel et al. 2013), loss of Scrib resulted in functional impairment of hematopoietic stem cells over serial transplantation and during stress (Mohr et al. 2018). Transcriptome profiling of Scrib- and Llgl1-deficient HSCs confirmed a minimal overlap of the respective transcriptional profiles, which is consistent with the diverging functional phenotypes. Interactome analysis of Scrib in hematopoietic cells informed about its involvement in cell motility and signaling but failed to confirm direct interaction with its putative Scribble complex partners.

In this study, we performed interactome analysis on Llgl1 in hematopoietic cells to assess for unique and overlapping interactions of Scrib and Llgl1 and to confirm and validate these functions in primary HSCs.

Materials and methods

Proteome binding partner analysis

The 3111 bp full length *M. musculus Llgl1* cDNA was amplified by PCR from a commercially available plasmid pYX-Asc (Source BioSciences, Nottingham, UK) using the following primers: Llgl1-F 5′-CACCAT GATGAAGTTTCGGTT-3′ and Llgl1-R 5′-TCACCC CAGAAAATCCT-3′. PCR fragments were gel-purified followed by directional cloning into pENTER/D-TOPO vector (Invitrogen, USA) as per the manufacture's protocol. From there, Llgl1 was subcloned in-frame into the destination vector pCeMM-NTAP(GS)-Gw (Center for Molecular Medicine of the Austrian Academy of Sciences, Vienna) mediated by LR recombination reaction. Production of retroviral particles and retroviral transduction of Ba/F3 cells with NTAP-Llgl1-GFP or NTAP-EmptyVector-GFP control was performed as described before (Heidel et al. 2012). Following retroviral infection, Ba/F3 cells expressing NTAP-Llgl1-GFP and NTAP-EmptyVector-GFP were GFP sorted by FACS and maintained in culture (RPMI1640 medium supplemented with 10% FBS, Thermo Fisher Scientific, USA) in a humid atmosphere of 5% at 37 °C. For binding partner analysis, protein complexes were purified using Streptavidin C1 Dynabeads MyOne (Invitrogen). In brief, 1×10^7 cells were lysed in 1 ml RIPA-buffer (50 mM TRIS/HCl, pH 7.5; 5 mM EDTA; 100 mM NaCl; 10 mM K2HPO4; 10% Glycerol; 1% Triton X-100; 0.5% NP40; protease- and phosphatase inhibitor mix) for 30 min on ice supported by 5 min ultrasonic disintegration. After centrifugation at 16,000×g for 10 min at 4 °C, the supernatant was collected and incubated with 50 µl Dynabeads MyOne-Streptavidin C1 for 8 h at 4 °C. Beads were sequentially washed with PBS, 1% NP40 followed by PBS, 0.1% NP40 followed by PBS, 0.5M NaCl followed by PBS and finally resuspended in 50 mM ammonium bicarbonate. Cysteines were reduced by adding 2 mM dithiothreitol (DTT) for 30 min at room temperature and subsequently β-methylthiolated by addition of 10 mM methyl methanethiosulfonate (MMTS). Digestion was performed by addition of 0.5 µg trypsin (Promega, Madison, WI, USA) and incubation overnight at 37 °C. Peptides were extracted by pooling the primary supernatant and the supernatant of a subsequent washing step using 0.1% (v/v) trifluoroacetic acid (TFA). Peptides were purified with reversed-phase C18 ZipTip nano-columns (Millipore, Burlington, MA, USA), eluted with 0.1% TFA/70% ACN, and dried. Protein identification was performed by high-resolution mass spectrometry on a hybrid dual-pressure linear ion trap/orbitrap mass spectrometer (LTQ Orbitrap Velos Pro, Thermo Scientific, San Jose, CA, USA) equipped with an EASY-nLC Ultra HPLC (Thermo Scientific). For analysis, peptide samples were adjusted to 10 µl 1% ACN/0.1% TFA and fractionated on a 75 µm (ID), 25 cm PepMap C18-column, packed with 2 µm resin (Dionex/Thermo Scientific). Separation was achieved through applying a

gradient from 2 to 35% ACN in 0.1% formic acid over 150 min at a flow rate of 300 nl/min. An Orbitrap full MS scan was followed by up to 15 LTQ MS/MS runs using collision-induced dissociation (CID) fragmentation of the most abundantly detected peptide ions. Essential MS settings were as follows: full MS (FTMS; resolution 60,000; m/z range 400–2000); MS/MS (Linear Trap; minimum signal threshold 500; isolation width 2 Da; dynamic exclusion time setting 30 s; singly charged ions were excluded from selection). Normalized collision energy was set to 35%, and activation time to 10 ms. Raw data processing and protein identification were performed using PEAKS Studio V.7.0 (Bioinformatics Solutions, Waterloo, Canada). False discovery rate was set to < 1%.

Flow cytometry and cell sorting

For immunophenotype analysis, bone marrow cells were resuspended in PBS/1% FBS after erythrocyte lysis (Pharm-Lyse™, BD Pharmingen, San Diego, CA). Sorting and analysis of LSK (Lin-Sca1 + Kit+) cells, CD34low expressing LSK cells (HSC) and CD34high expressing LSK cells (MPP) were performed as previously described (Heidel et al. 2013, 2012). Unless otherwise stated, the following antibodies were used: biotinylated antibodies against Gr-1 (RB6-8C5), B220 (RA3-6B2), CD19 (6D5), CD3 (145-2C11), CD4 (GK1.5), CD8 (53-6.7), TER119 and IL7Ra (A7R34) (all Biolegend, SanDiego, CA, USA) were used for lineage staining. An APC-Cy7- or BV421-labeled streptavidin-antibody (Biolegend) was used for secondary staining together with an APC-anti-KIT (clone 2B8), a PE-Cy7- or PE-anti-Sca-1 antibody (clone E13-161.7), and a CD34-FITC (Becton Dickinson). Cells were FACS sorted using a BD FACSAria Fusion (Becton Dickinson). Analysis was performed using FlowJo™ software (Treestar, Ashland, OR).

Cell motility and migration assay

LSK cells were sorted from conditional Scrib or Llgl1 knockout mice 11 days after the last pIpC injection. Sorted LSK cells were incubated in serum-free buffer (SFEM medium, STEMCELL Technologies) for 2 h to reduce the stress after the sorting. Next, 1×10^4 cells were plated on RetroNectin™ coated 35 mm glass bottom dishes (WPI) and motility was recorded using an Axiovert 200 m microscope (Zeiss MicroImaging GmbH, Jena, Germany) equipped with a live cell imaging incubator (Okolab, Ottaviano, Na, Italy) and a motorized stage (Märzhäuser

Wetzlar GmbH & Co. KG, Wetzlar, Germany) for 15–16 h at 37 °C and 5% CO_2. In each time series, several fields of view of two glass bottom dishes per condition were observed using the MarkandFind function in the Zeiss Axiovision software. Image analysis was performed using the tracking function in Image-Pro Plus 6. Several tracks per field of view were summarized and used for further analysis. Chemotaxis experiments to assess for migratory capacity were performed using 96-well 6.5 mm transwell plates (5 μm pore size Costar, Corning, NY). Plates were coated on the lower chamber overnight with retronectin at 4 °C. After washing with PBS, the transwell membrane chamber was carefully placed into 96-well plates. The lower reservoir of the chambers was filled with 100 μl of SFEM with or without recombinant murine SDF-1α (100 ng/ml, R & D Systems, Inc., Minneapolis, MN). Briefly, 100 μl of serum-free chemotaxis medium containing 5×10^3 HSCs (CD34^{low} LSK) or MPPs (CD34^{high} LSK) cells derived from Llgl1$^{+/+}$ or Llgl1$^{-/-}$ and Scrib$^{+/+}$ or Scrib$^{-/-}$ mice were seeded in the upper chambers. Migration of HSCs or MPPs was allowed to continue for 4 h at 37 °C, 5% CO_2. After incubation, the upper chamber was removed and the migrated cells from the lower chambers were collected, visualized and manually counted under the microscope.

Static adhesion assay

Adhesion assays were performed on 96-well plates coated with retronectin (Takara Clontech, USA) or blocked with 1% BSA at 4 °C overnight. Next, 1×10^3 FACS sorted HSCs (CD34^{low} LSK) or MPPs (CD34^{high} LSK) from Llgl1$^{+/+}$ or Llgl1$^{-/-}$ and Scrib$^{+/+}$ or Scrib$^{-/-}$ mice were resuspended in SFEM medium and seeded per well onto the retronectin-coated plates for 1 h at 37 °C. Non-adherent cells were removed by three consecutive washing steps at room temperature using HBSS (Thermo Fisher Scientific) and adherent cells were counted under the microscope. Results are represented as percentage of adherent cells.

Mouse models

All mice were housed under pathogen-free conditions in the accredited Animal Research Facility of the Otto-von-Guericke University—Medical Faculty, Magdeburg. All experiments were conducted after approval by the Landesverwaltungsamt Saxony-Anhalt. Conditional Scrib knockout (KO) mice have been generated as described before (Hartleben et al. 2012) with Scrib exons 2–8 being

flanked with loxP sites. Mice harboring a floxed (flanked with loxP sites) allele of Llgl1 have been generated as previously described (Klezovitch et al. 2004). Exon 2 (the exon downstream from the exon with the first ATG codon) was flanked by LoxP sequences, and the beta-geo selectable marker was removed by transient expression of Cre-recombinase in the embryonic stem cells. Both strains of mice have been backcrossed in more than eight generations into a C57BL/6 background. Conditional Scrib- and Llgl1-KO mice were crossed with transgenic Mx1-Cre mice to make them inducible—as described before (Heidel et al. 2013; Klezovitch et al. 2004; Mohr et al. 2018). Mx1-Cre-recombinase was induced by intraperitoneal injections of low-molecular weight poly-I-poly-C (pIpC) and excision was confirmed by PCR.

Intravital 2-photon microscopy

Whole bone marrow cells were collected from conditional knockout mice after genetic inactivation of Scribble or Llgl1 (as described above), stained with biotin-conjugated lineage cocktail antibodies and subjected to lineage depletion using magnetic beads (Streptavidin Particles Plus-DM, BD Biosciences) and LSK cells were isolated by FACS sorting. Non-irradiated Col2.3-GFP reporter mice (GFP expression is under the control of the Col2.3 promoter labeling osteoblastic cells) were each injected with 5×10^4 wildtype or KO LSK cells labeled with the Cell Tracker orange CMTMR dye (C2927, Thermo Fisher Scientific, Darmstadt) at a final concentration of 10 uM for 30 min at 37 °C. The mice were anesthetized by xylene/ketamine and prepared as described before (Lo Celso et al. 2009). In brief, the calvarial bone marrow cavity was visualized using a 20× objective on a 2-photon microscope (LaVision Biotech, Bielefeld). For three-dimensional analysis of the bone marrow cavity, z stacks were acquired with a z-step of 2 μm using the Inspector Pro Software. Distances between CMTMR labeled cells and bone or osteoblastic cells, as well as total path length were measured in the image stacks by ImageJ as described (Lo Celso et al. 2009).
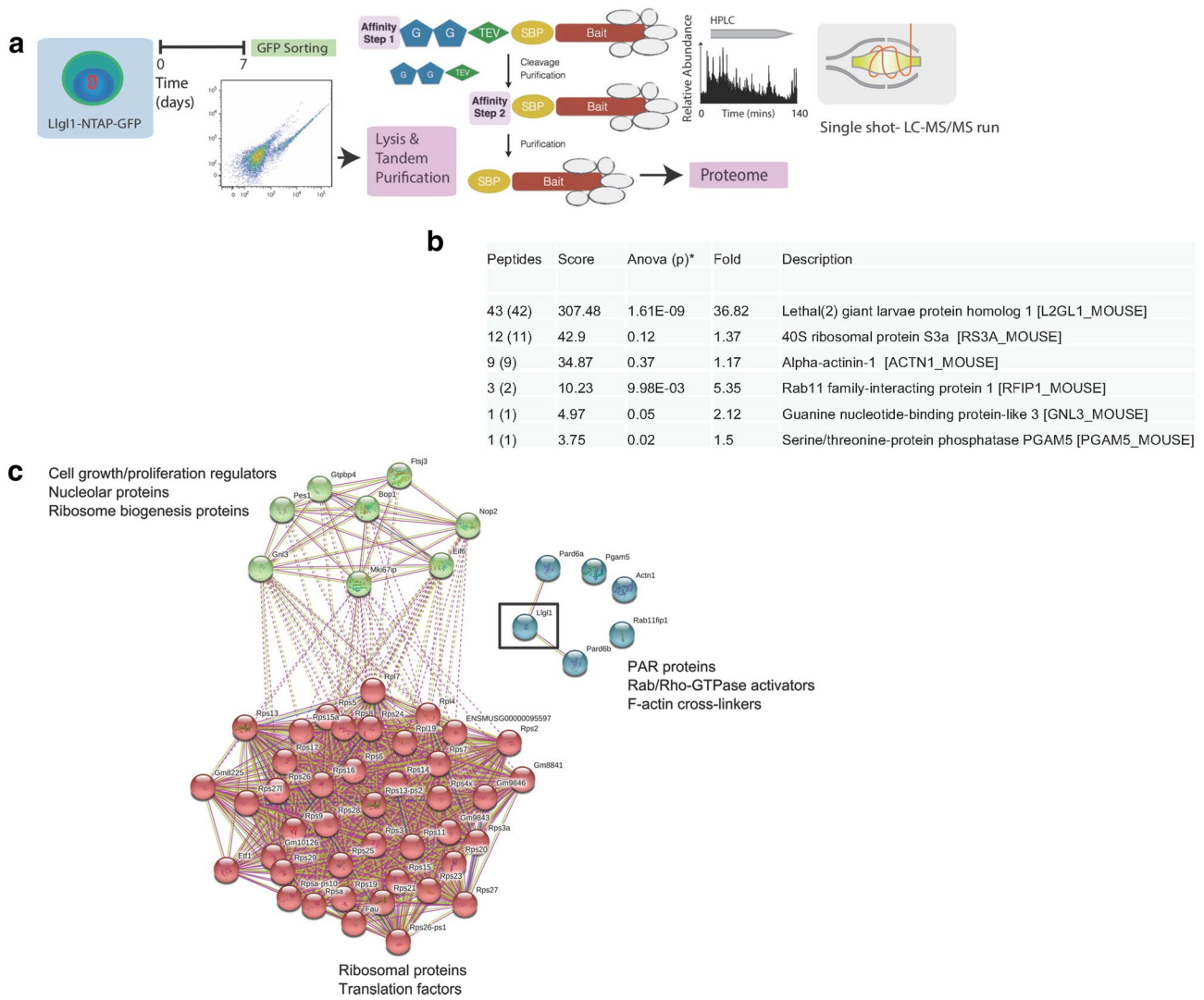
Statistical analysis

Graphs were analyzed using GraphPad Prism Version 6 (GraphPad Software Inc., La Jolla, CA, USA). Statistical significance was determined using a t test or the Mann–Whitney U test (when normal distribution was not given). p value less than 0.05 was considered statistically significant ($p < 0.05$ indicated as *, $p < 0.01$ indicated as **, $p < 0.001$ indicated as *** and $p < 0.0001$ indicated as ****).

Results and discussion

Scrib- but not Llgl1-binding partners are linked with cell motility and adhesion

In our previous work, we have defined functional roles for the cell fate determinants Llgl1 (Heidel et al. 2013) and Scrib (Mohr et al. 2018) in hematopoietic stem cells. While genetic inactivation of Llgl1 resulted in increased fitness and enhanced self-renewal, deletion of Scrib led to a functional decrease and depletion of HSCs during serial transplantation and under stress. Of note, transcriptional profiling of HSCs showed minimal overlap between Scrib- and Llgl1-deficient stem cells. Binding partner analysis of Scrib in murine hematopoietic cells (Mohr et al. 2018) using affinity purification followed by mass spectrometry confirmed functional roles in cell signaling, adhesion and motility; however, none of the identified binding partners included polarity modules as described in drosophila. As both cell fate determinants, Scrib and Llgl1 have been linked with functional roles regarding adhesion and migration in other model systems, we sought to assess whether these cellular functions are shared in hematopoietic cells between the putative complex partners Scrib and Llgl1. As described for Scribble protein before, we expressed Llgl1 in hematopoietic cells using a vector system that enables tandem affinity purification (TAP). In this system, a fusion protein is created that harbors a designed tandem affinity purification tag (Fig. 1a). Analysis of precipitated CeMM-NTAP-Llgl1 versus empty vector by mass spectrometry revealed 6 putative binding partners (Fig. 1b), compared to 27 identified Scrib binding partners in the same model system (Mohr et al. 2018). Analysis of the binding partner network using the STRING database (Szklarczyk et al. 2017) of known and predicted protein–protein interactions (http://www.string-db.org) that include regulators of cell growth and proliferation, ribosomal proteins, translation factors, cytoskeletal proteins, Rho-GTPase activators and Llgl1 itself (Fig. 1c). Binding of Scrib to Llgl1 could not be detected. Inversely, Llgl1 had not been detected in Scrib interactome analysis either (Mohr et al. 2018). However, binding to Rac/Rho-GTPase activator RFIP1 links Llgl1 with the Par complex, which may indicate a conserved functional link in hematopoietic cells.

To understand shared and unique interactions of Scrib and Llgl1 in hematopoietic cells, we analyzed the overlap of predicted and proven interactions of both proteins by STRING analysis. Shared cellular functions included protein synthesis, ribosome biogenesis, proliferation, differentiation and cell signaling (Fig. 2). Functions that appeared exclusively linked with the Llgl1 interactome comprised Par

Peptides	Score	Anova (p)*	Fold	Description
43 (42)	307.48	1.61E-09	36.82	Lethal(2) giant larvae protein homolog 1 [L2GL1_MOUSE]
12 (11)	42.9	0.12	1.37	40S ribosomal protein S3a [RS3A_MOUSE]
9 (9)	34.87	0.37	1.17	Alpha-actinin-1 [ACTN1_MOUSE]
3 (2)	10.23	9.98E-03	5.35	Rab11 family-interacting protein 1 [RFIP1_MOUSE]
1 (1)	4.97	0.05	2.12	Guanine nucleotide-binding protein-like 3 [GNL3_MOUSE]
1 (1)	3.75	0.02	1.5	Serine/threonine-protein phosphatase PGAM5 [PGAM5_MOUSE]

Fig. 1 Binding partner analysis of Llgl1 in hematopoietic cells by mass spectrometry. **a** Experimental scheme for expression of Llgl1 in a tandem affinity purification (TAP) tag vector system in murine cell lines followed by immunoprecipitation, purification and mass spectrometry analysis. **b** Identified binding partners of Llgl1 in murine hematopoietic cells. Depicted are matched peptides identified and protein names. **c** Interactions between Llgl1 and its binding partners are depicted using STRING database analysis (http://string-db. org/). The network was constructed using six identified candidate protein names as input, with medium confidence threshold parameter of 0.4. The identified interaction network grouped into 3 (k-means clustering) clusters containing functional associations (direct and indirect) specifically highlighted. The solid and dotted lines indicate connection within the same and different cluster, respectively. Different line colors represent the types of evidence for the association (Pink—experimentally determined; Blue—gene co-occurrence; yellow—derived from text-based data analysis)

complex members, actin assembly, cell cycle regulation and cellular stress responses. In contrast, functions exclusively linked with Scrib included cell metabolism, actin remodeling, adaptor associated proteins, migration and adhesion. Scrib has been described to be critically involved in maintenance of cellular orientation and integrity in drosophila, neuronal tissue and epithelial cells (Humbert et al. 2006). In mammalian hematopoietic cells, deletion of Scrib affected T-cell polarization and function (Pike et al. 2011). As cellular orientation and polarization are involved in adhesion and migration of hematopoietic cells, we aimed to functionally validate these functions in Scrib-deficient hematopoietic stem cells.
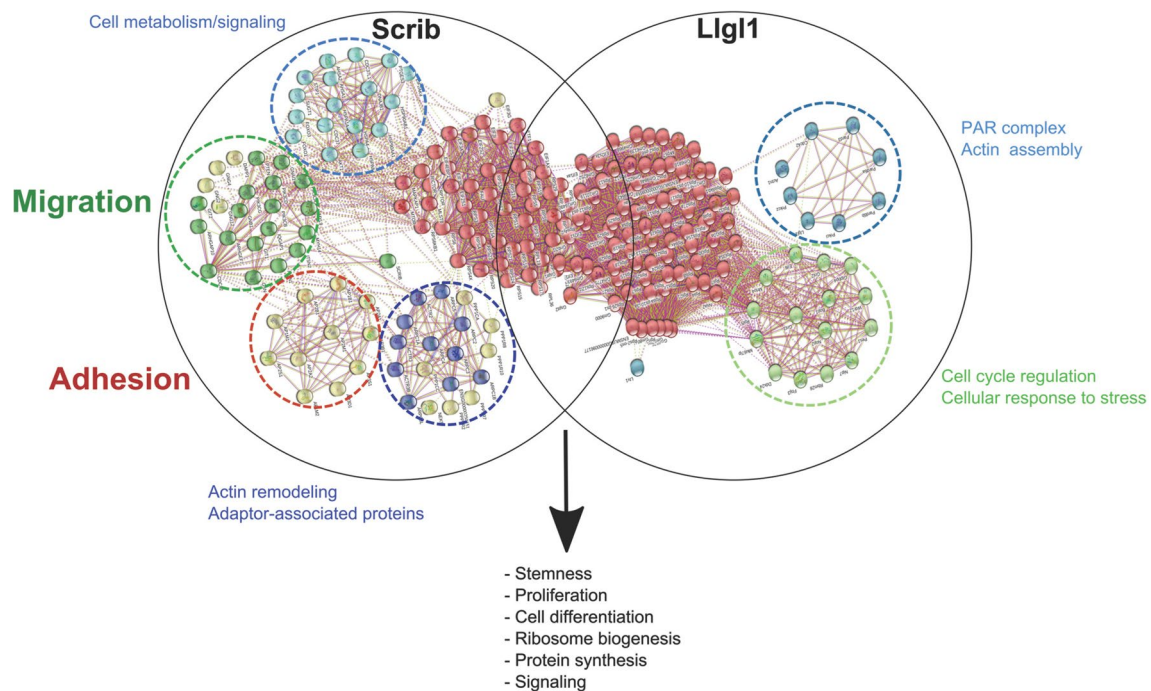
Fig. 2 Protein interactome network and comparison of predicted functions shared between Scrib and Llgl1. Venn diagram depicting the interactomes of Scrib (left) and Llgl1 (right), which partly overlap (shared functions). The STRING database was used to establish functional associations among the known and predicted proteins using training protein names as query for Scrib and Llgl1 interaction network, with minimal confidence score of 0.4. Different line colors represent the types of evidence in predicting the association; blue line—co-occurrence evidence; pink line—experimental evidence; yellow line—text mining evidence. The interacting proteins have been clustered (k-means clustering) based on their functions and associations. The continuous and dotted lines represent direct (physical) and indirect (functional) interactions within the same and with the other clusters. Clusters of functionally related nodes were manually circled and labeled. The common hits between Scrib and Llgl1 interactome network are highlighted, whereas the unique functions that are categorized as members of the same protein complex or biological processes (e.g., adhesion, migration, cytoskeleton network) are highlighted by the colored labels

In vitro motility of murine HSPC is not affected by genetic deletion of Scrib or Llgl1

To investigate stem- and progenitor cell function, we sorted HSCs and MPPs from bone marrow of conditional Scrib- and Llgl1 knockout mice, respectively. Cells were sorted 11 days following the last poly-I-poly-C injection to enable recovery from interferon response. The HSPC population was defined as Lineage-negative, Sca-1-positive, Kit-positive (LSK) cells, while cell population enriched for hematopoietic stem cells (HSC) was defined as CD34low LSK cells and multipotent progenitor (MPP) enriched cells were defined as CD34high LSK cells (Fig. 3a). First, we aimed to investigate, whether genetic deletion of Scribble or Llgl1 resulted in changes of undirected cell motility. LSK cells incubated in SFEM medium supplemented with cytokines (as described above) were recorded for 15–16 h using an Axiovert200m microscope. Interestingly, we found no significant deregulation of cell motility following inactivation of either Scribble complex member (Scrib or Llgl1). Scrib-deficient HSCs showed a slight increase and Llgl1-deficient HSCs a moderate increase in cell motility after seeding the cells into the respective wells (Fig. 3 b, c). However, this effect disappeared over time and motility was comparable to the respective wildtype controls (Scrib$^{+/+}$ or Llgl1$^{+/+}$ HSPCs, respectively).

Undirected motility may depend to a minor extent on proteins orchestrating the polarity network of Rho-GTPases and the actin/myosin filaments. One example underlining this observation is the fast moving and turning of specific immune cells that do not have a highly organized cytoskeleton and tend to adhere weakly. In contrast, hematopoietic stem cells may depend to a higher degree on the polarity network, which is required for proper localization, migration and asymmetric division (Florian et al. 2012; Giebel and Bruns 2008). Therefore, we aimed to

Fig. 3 Cell motility analysis of Scrib- and Llgl1-deficient HSPCs. **a** Representative flow cytometry plot depicting sorting of murine HSPCs. BM obtained from femurs and tibias of Scrib$^{+/+}$ or Scrib$^{-/-}$ and Llgl1$^{+/+}$ or Llgl1$^{-/-}$ mice, respectively, was lineage depleted, stained and flow sorted to obtain LSK (lineage-, Kit+, Sca-1+) cells, HSC enriched LSKs (CD34low LSK) or MPP enriched LSKs (CD34high LSK). **b, c** Sorted cells were incubated in SFEM medium with cytokines and basic cell motility was assessed using several fields of view per 35 mm glass bottom dish with 1×10^4 pooled Scrib$^{+/+}$ or Scrib$^{-/-}$ and Llgl1$^{+/+}$ or Llgl1$^{-/-}$ mice LSK cells. Each field of view was imaged repeatedly during a 15–16 h time period. Phase contrast images were then used to extract the single cell tracks for distance analysis. Summarized tracks are shown here as mean displacement per frame
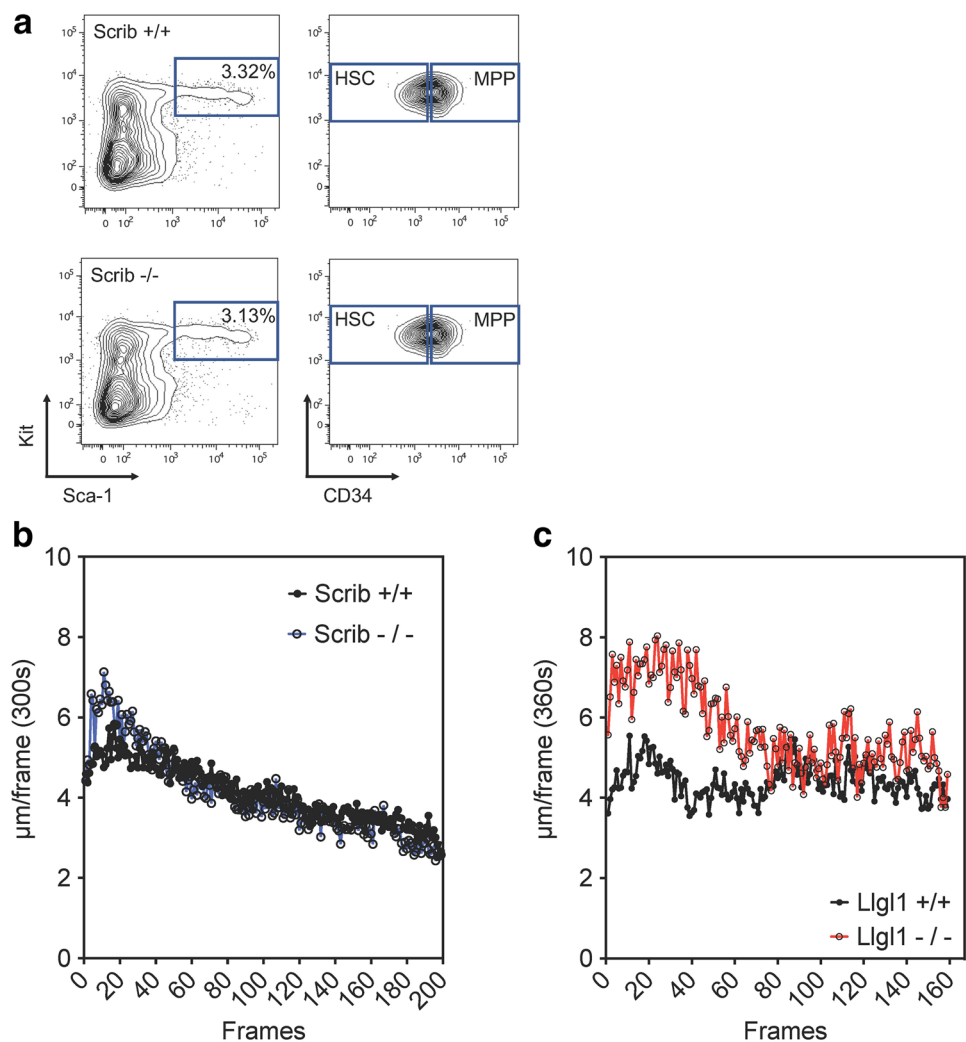

assess for adhesion and directed migration of Scrib- and Llgl1-deficient HSCs.

Static adhesion of HSC and MPP is increased following inactivation of Scrib but not Llgl1

To assess for potential alterations in cell adhesion of HSPCs, we conducted a static adhesion assay using sorted HSC and MPP from Scrib- and Llgl1-knockout mice, respectively. Following cell sorting, 1×10^3 HSCs (CD34low LSK) or MPPs (CD34high LSK) from Llgl1$^{+/+}$ or Llgl1$^{-/-}$ and Scrib$^{+/+}$ or Scrib$^{-/-}$ mice were seeded on RetroNectin-coated plates and incubated for 1 h to enable attachment to the plate. After the first washing step, Scrib-deficient HSCs showed significant increase in cell adhesion compared to Scrib$^{+/+}$ controls (Fig. 4a, $p = 0.0043$**). During sequential washing steps this effect was maintained. Likewise, higher numbers of Scrib$^{-/-}$ MPPs adhered to

the RetroNectin-coated surface after the first (Fig. 4b, $p = 0.0247$*) and following ($p = 0.0009$***) washing steps. In contrast, genetic deletion of Llgl1 did not result in alteration of cell adhesion to RetroNectin. This was detectable in both Llgl1$^{-/-}$ HSCs (Fig. 4c, $p = 0.4298$ at 1st wash) and MPPs (Fig. 4d, $p = 0.5737$ at 1st wash) when compared to the respective Llgl1$^{+/+}$ controls. These findings indicate, for the first time, that loss of Scrib may result in alteration of hematopoietic stem- and progenitor-cell adhesion. Alteration of cell adhesion may influence localization of hematopoietic stem- and progenitor cells in the niche and also their migratory capacity. Both, localization and migration of stem cells have been described to be relevant for stem cell function and self-renewal capacity (Boulais and Frenette 2015). Impaired mobilization of HSCs from the bone marrow following cytotoxic stimuli (such as 5-FU) may eventually result in impaired stress responses and decreased survival following irradiation or chemotherapy

Fig. 4 Altered adhesion of Scrib- and Llgl1-deficienct HSPCs. **a, c** Static adhesion of hematopoietic stem cells (CD34low LSK) and **b, d** multipotent progenitors (CD34high LSK) to RetroNectin (rn). Isolated HSC and MPP cells were serum starved and plated in 96-well plates coated with rn or BSA (control). The percentage of adherent cells from Scrib$^{+/+}$ or Scrib$^{-/-}$ and Llgl1$^{+/+}$ or Llgl1$^{-/-}$ mice was calculated after 1 h incubation (37 °C, 5% CO_2) and compared relative to wildtype controls. Data is depicted as mean ± SEM of two independent experiments per genotype performed in triplicate (ns, not significant; *$p < 0.05$; **$p < 0.01$)
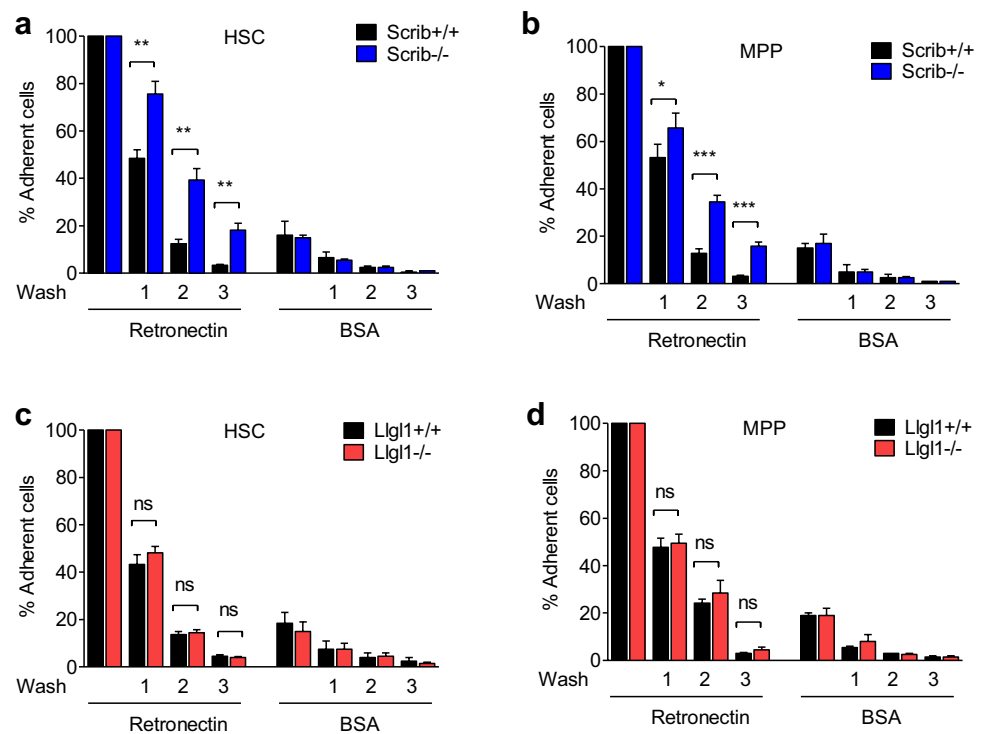
as observed for Scrib-deficient hematopoiesis (Mohr et al. 2018).

Scrib-deficient HSCs reveal impaired migratory capacity in vitro and in vivo

To assess the migratory capacity of hematopoietic stem cells, we conducted chemotaxis experiments against an SDF1alpha gradient in vitro. Scrib- or Llgl1-deficient HSCs or MPPs (and the respective Scrib$^{+/+}$ or Llgl1$^{+/+}$ controls) were sorted and 5×10^3 cells were seeded in transwell chambers to allow migration against the SDF1alpha gradient. Migrated cells were counted after 4 h of incubation. After conditional Scrib deletion, we found a significant reduction of the migratory capacity of Scrib$^{-/-}$ HSCs (Fig. 5a, $p = 0.0049$**) compared to Scrib$^{+/+}$ controls. Likewise, the number of migrated Scrib$^{-/-}$ MPPs (Fig. 5b, $p = 0.0030$**) appeared significantly reduced. In contrast, Llgl1-deficient HSCs (Fig. 5c) or MPPs (Fig. 5d) did not reveal any significant reduction in migratory capacity when compared to the respective Llgl1$^{+/+}$ controls. These results support the hypothesis, that increased adhesiveness of Scrib-deficient HSCs and MPPs may eventually result in a migratory defect. However, assessment of migratory capacity ex vivo in a transwell plate against a rather high SDF1alpha gradient may create secondary dependency of HSCs on a cell fate determinant as Scrib due to the

culturing conditions and may therefore lead to overestimation of the phenotype. Therefore, we aimed to assess stem cell migration and localization in the bone marrow niche by intravital microscopy.

To validate our findings and to assess for the dependency of HSPCs on Scrib in vivo, we performed intravital imaging of murine hematopoietic stem- and progenitor cells. We induced conditional deletion of Scrib by pIpC injections into Scrib flox/flox Mx + mice and Scrib$^{+/+}$ Mx + controls. Our previous data had shown that abundance of murine HSCs was not significantly altered following genetic deletion of Scrib at 4 months post pIpC. However, cells showed a clear functional decline when serially transplanted into primary or secondary recipient mice (Mohr et al. 2018). To avoid a potential selection bias, we harvested bone marrow cells early (11 days after pIpC injection), which may avoid further functional decrease over time but allows for partial recovery of HSCs after the pIpC induced interferon response (Essers et al. 2009; Pietras et al. 2014; Walter et al. 2015). As both HSCs and MPPs had shown differences in stem cell migration and adhesion, we decided to sort LSK cells (rather than separate sorting of HSCs and MPPs) from Scrib$^{+/+}$ or Scrib$^{-/-}$ mice to obtain sufficient cell numbers for transplantation. Intravital imaging (Fig. 6a) revealed similar localization of murine Scrib$^{-/-}$ HSPCs to the endosteum, as compared to Scrib$^{+/+}$ controls (Fig. 6b,
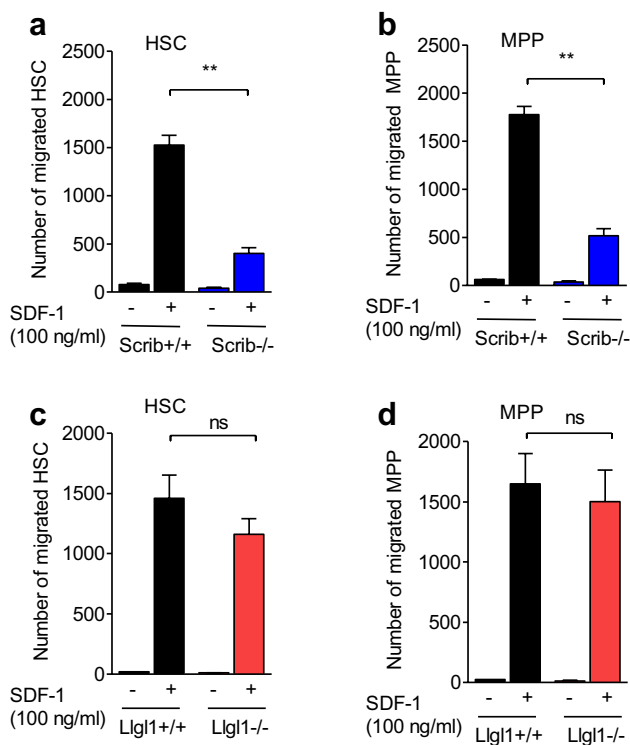
Fig. 5 Changes in directed migration of Scrib- and Llgl1-deficient HSPCs. **a, b** Chemotaxis assay investigating migration of HSCs and MPPs isolated from Scrib$^{+/+}$ or Scrib$^{-/-}$ and **c, d** Llgl1$^{+/+}$ or Llgl1$^{-/-}$ mice. Cells were serum starved and subsequently seeded in the upper part of a transwell chamber in the presence or absence of 100 ng/ml SDF-1alpha in the lower compartment. Cells in the lower chamber were counted after 4 h incubation (37 °C, 5% CO2). Data are presented as mean ± SD of 2 independent experiments per genotype, performed in duplicate (*$p < 0.05$)

Overall, path length per stack of Scrib$^{-/-}$ HSPCs was significantly shorter compared to Scrib$^{+/+}$ controls (Fig. 6e, $p = 0.0285$*). These results recapitulate our in vitro findings and confirm a defect of Scrib-deficient HSPCs in their migratory capacity.

Inactivation of Scrib has been linked with loss of migratory capacity of various cell types. Loss of Scrib contributed to failure of dorsal closure in the drosophila embryo (Bilder et al. 2000) and also murine embryonic fusion events (Murdoch et al. 2003). This function appears to be conserved in adult murine and human epithelial cells, where Scrib is required for sheet migration during wound healing (Dow et al. 2007). Motility and polarity of murine T-cells are also influenced by inactivation of Scrib (Ludford-Menting et al. 2005). However, the functional role of the Scribble complex in regulating cell migration seems to be also context-dependent (Humbert et al. 2006). Our data indicates that this function of the Scribble complex appears to be conserved in murine HSCs for Scrib but not Llgl1. While genetic deletion of Scrib impairs the migratory capacity of HSPCs in vitro and in vivo, inactivation of Llgl1 did not reveal a major function in motility, adhesion or migration. This finding is in contrast to the role of Llgl1 in other cell types (Arquier et al. 2001; Humbert et al. 2006; Manfruelli et al. 1996), where Llgl1 inactivation results in alteration of cell migration and invasiveness.

Disturbance of HSC migration after genetic deletion of Scrib as shown herein may, in part, also explain the functional impairment of Scrib-deficient HSCs in vivo (Mohr et al. 2018). Recently, alteration of migratory capacity has been linked with disturbance of HSC self-renewal and niche localization (Lhoumeau et al. 2016; Prashad et al. 2015). As shown before, Scrib influences Rho-GTPases activity through interaction with GTPase activators (Mohr et al. 2018). This interaction may also explain the impact of Scrib on HSC migration and function, as extensive characterization of Rho-GTPases, such as CDC42, have shown significant influence on HSC fitness and self-renewal capacity (Florian et al. 2013; Yang et al. 2007).

Taken together, our data provides the first evidence for a functional role of Scrib but not Llgl1 in HSC adhesion and migration, which may explain the relevance of Scrib for maintenance of HSC function in vivo.

$p = 0.11$). Likewise, the distance to the osteoblastic cells appeared to be not significantly different (Fig. 6c); however, there was a trend towards an increased distance of Scrib-deficient HSPCs ($p = 0.0531$). To analyze migratory capacity in vivo, we performed cell traveling path analysis (Fig. 6d, e). Of note, comparable numbers of Scrib$^{+/+}$ and Scrib$^{-/-}$ HSPCs were detectable in the bone marrow of recipient mice, which is an indicator of undisturbed homing capacity. When we analyzed the average traveling path, Scrib$^{-/-}$ HSPC traveling appeared less complex than that of Scrib$^{+/+}$ controls (Fig. 6d; representative plots).

Fig. 6 Time-lapse intravital microscopy of Scrib- and Llgl1-deficient HSPCs. **a** Schematic model representing intravital imaging of the calvarium. LSK cells (CMTMR labeled) were transplanted into non-irradiated recipients (2 independent cohorts, $n=2$ mice per genotype). Imaging was performed within 5 h of transplantation. Bone collagen SHG (blue), GFP-positive osteoblastic cells (green), HSPC (red). **b, c** Shortest distances in 3D of HSPC to the endosteum (left panel) and to the osteoblastic cells (right panel) were measured in wildtype and Scrib$^{-/-}$ non-irradiated recipients (Error bars represent means $\pm$ SEM, $n=50$ cells per genotype, $p=0.11$, endosteum, $p=0.0531$, osteoblastic cell). **d** Representative spidergrams indicating the paths of migrating Scrib$^{+/+}$ (upper panel) or Scrib$^{-/-}$ (lower panel) HSPCs are shown. **e** Migration of Scrib$^{+/+}$ and Scrib$^{-/-}$ HSPCs as indicated by average path length (error bars represent mean $\pm$ SEM, $n=22$ cells per genotype, *$p<0.05$)

Author contributions BPD, JM, CK, TMS, CH, SG, CZ, FP and TK performed experiments and analyzed data. MN, BH, TH and GW provided material. TH, TK, DSK and FHH analyzed data and provided material. TK and BPD contributed to the writing of the manuscript. FHH supervised the research and wrote the paper.

Compliance with ethical standards

Conflict of interest None.

Ethical approval This study does not involve any human samples or material. All animal experiments were conducted after approval by the Landesverwaltungsamt Saxony-Anhalt.

References

Althoff MJ et al (2017) Scribble controls HSC self-renewal through polarity-dependent activation of the hippo signaling pathway. Blood 130:710

Arquier N, Perrin L, Manfruelli P, Semeriva M (2001) The Drosophila tumor suppressor gene lethal(2)giant larvae is required for the emission of the Decapentaplegic signal. Development 128:2209–2220

Bilder D, Li M, Perrimon N (2000) Cooperative regulation of cell polarity and growth by Drosophila tumor suppressors. Science 289:113–116

Boulais PE, Frenette PS (2015) Making sense of hematopoietic stem cell niches. Blood 125:2621–2629. https://doi.org/10.1182/blood-2014-09-570192

Dow LE et al (2007) The tumour-suppressor Scribble dictates cell polarity during directed epithelial migration: regulation of Rho GTPase recruitment to the leading edge. Oncogene 26:2272–2282. https://doi.org/10.1038/sj.onc.1210016

Essers MA, Offner S, Blanco-Bose WE, Waibler Z, Kalinke U, Duchosal MA, Trumpp A (2009) IFNalpha activates dormant haematopoietic stem cells in vivo. Nature 458:904–908. https://doi.org/10.1038/nature07815

Florian MC et al (2012) Cdc42 activity regulates hematopoietic stem cell aging and rejuvenation. Cell Stem Cell 10:520–530. https://doi.org/10.1016/j.stem.2012.04.007

Florian MC et al (2013) A canonical to non-canonical Wnt signalling switch in haematopoietic stem-cell ageing. Nature 503:392–396. https://doi.org/10.1038/nature12631

Giebel B, Bruns I (2008) Self-renewal versus differentiation in hematopoietic stem and progenitor cells: a focus on asymmetric cell divisions. Curr Stem Cell Res Ther 3:9–16

Hartleben B et al (2012) Role of the polarity protein Scribble for podocyte differentiation and maintenance. PLoS One 7:e36705. https://doi.org/10.1371/journal.pone.0036705

Hawkins ED et al (2013) Regulation of asymmetric cell division and polarity by Scribble is not required for humoral immunity. Nat Commun 4:1801. https://doi.org/10.1038/ncomms2796

Hawkins ED et al (2014) Lethal giant larvae 1 tumour suppressor activity is not conserved in models of mammalian T and B cell leukaemia. PLoS One 9:e87376. https://doi.org/10.1371/journal.pone.0087376

Hawkins ED, Oliaro J, Ramsbottom KM, Newbold A, Humbert PO, Johnstone RW, Russell SM (2016) Scribble acts as an oncogene in Emu-myc-driven lymphoma. Oncogene 35:1193–1197. https://doi.org/10.1038/onc.2015.167

Heidel FH et al (2012) Genetic and pharmacologic inhibition of beta-catenin targets imatinib-resistant leukemia stem cells in CML. Cell Stem Cell 10:412–424. https://doi.org/10.1016/j.stem.2012.02.017

Heidel FH et al (2013) The cell fate determinant Llgl1 influences HSC fitness and prognosis in AML. J Exp Med 210:15–22. https://doi.org/10.1084/jem.20120596

Heidel FH, Arreba-Tutusaus P, Armstrong SA, Fischer T (2015) Evolutionarily conserved signaling pathways: acting in the shadows of acute myelogenous leukemia's genetic diversity. Clin Cancer Res 21:240–248. https://doi.org/10.1158/1078-0432.CCR-14-1436

Humbert PO, Dow LE, Russell SM (2006) The Scribble and par complexes in polarity and migration: friends or foes? Trends Cell Biol 16:622–630. https://doi.org/10.1016/j.tcb.2006.10.005

Humbert PO, Grzeschik NA, Brumby AM, Galea R, Elsum I, Richardson HE (2008) Control of tumourigenesis by the Scribble/Dlg/Lgl polarity module. Oncogene 27:6888–6907. https://doi.org/10.1038/onc.2008.341

Klezovitch O, Fernandez TE, Tapscott SJ, Vasioukhin V (2004) Loss of cell polarity causes severe brain dysplasia in Lgl1 knockout mice. Genes Dev 18:559–571. https://doi.org/10.1101/gad.1178004

Knoblich JA (2010) Asymmetric cell division: recent developments and their implications for tumour biology. Nat Rev Mol Cell Biol 11:849–860. https://doi.org/10.1038/nrm3010

Lhoumeau AC et al (2016) Ptk7-deficient mice have decreased hematopoietic stem cell pools as a result of deregulated proliferation and migration. J Immunol 196:4367–4377. https://doi.org/10.4049/jimmunol.1500680

Lo Celso C et al (2009) Live-animal tracking of individual haematopoietic stem/progenitor cells in their niche. Nature 457:92–96. https://doi.org/10.1038/nature07434

Ludford-Menting MJ et al (2005) A network of PDZ-containing proteins regulates T cell polarity and morphology during migration and immunological synapse formation. Immunity 22:737–748. https://doi.org/10.1016/j.immuni.2005.04.009

Manfruelli P, Arquier N, Hanratty WP, Semeriva M (1996) The tumor suppressor gene, lethal(2)giant larvae (1(2)g1), is required for cell shape change of epithelial cells during Drosophila development. Development 122:2283–2294

Mohr J et al (2018) The cell fate determinant Scribble is required for maintenance of hematopoietic stem cell function. Leukemia 32:1211–1221. https://doi.org/10.1038/s41375-018-0025-0

Murdoch JN et al (2003) Disruption of scribble (Scrb1) causes severe neural tube defects in the circletail mouse. Hum Mol Genet 12:87–98

Pietras EM, Lakshminarasimhan R, Techner JM, Fong S, Flach J, Binnewies M, Passegue E (2014) Re-entry into quiescence protects hematopoietic stem cells from the killing effect of chronic exposure to type I interferons. J Exp Med 211:245–262. https://doi.org/10.1084/jem.20131043

Pike KA, Kulkarni S, Pawson T (2011) Immature T-cell clustering and efficient differentiation require the polarity protein Scribble. Proc Natl Acad Sci USA 108:1116–1121. https://doi.org/10.1073/pnas.1018224108

Prashad SL et al (2015) GPI-80 defines self-renewal ability in hematopoietic stem cells during human development. Cell Stem Cell 16:80–87. https://doi.org/10.1016/j.stem.2014.10.020

Sengupta A et al (2011) Atypical protein kinase C (aPKCzeta and aPKClambda) is dispensable for mammalian hematopoietic stem cell activity and blood formation. Proc Natl Acad Sci USA 108:9957–9962. https://doi.org/10.1073/pnas.1103132108

Szklarczyk D et al (2017) The STRING database in 2017: quality-controlled protein-protein association networks made broadly accessible. Nucleic Acids Res 45:D362–D368. https://doi.org/10.1093/nar/gkw937

Walter D et al (2015) Exit from dormancy provokes DNA-damage-induced attrition in haematopoietic stem cells. Nature 520:549–552. https://doi.org/10.1038/nature14131

Yang L, Wang L, Geiger H, Cancelas JA, Mo J, Zheng Y (2007) Rho GTPase Cdc42 coordinates hematopoietic stem cell quiescence and niche interaction in the bone marrow. Proc Natl Acad Sci USA 104:5091–5096. https://doi.org/10.1073/pnas.0610819104